HHS Public Access

Author manuscript

*Science*. Author manuscript; available in PMC 2020 February 03.

Published in final edited form as:

*Science*. 2019 December 06; 366(6470): 1218–1225. doi:10.1126/science.aay4509.

# Stem cell–driven lymphatic remodeling coordinates tissue regeneration

**Shiri Gur-Cohen**[1], **Hanseul Yang**[1], **Sanjeethan C. Baksh**[1], **Yuxuan Miao**[1], **John Levorse**[1], **Raghu P. Kataru**[2], **Xiaolei Liu**[3], **June de la Cruz-Racelis**[1], **Babak J. Mehrara**[2], **Elaine Fuchs**[1,*]

[1]Howard Hughes Medical Institute, Robin Chemers Neustein Laboratory of Mammalian Cell Biology and Development, The Rockefeller University, New York, NY 10065, USA.

[2]Department of Surgery, Plastic and Reconstructive Surgery Service, Memorial Sloan Kettering Cancer Center, New York, NY 10065, USA.

[3]Center for Vascular and Developmental Biology, Feinberg Cardiovascular and Renal Research Institute, Northwestern University, Chicago, IL 60611, USA.

## Abstract

Tissues rely on stem cells (SCs) for homeostasis and wound repair. SCs reside in specialized microenvironments (niches) whose complexities and roles in orchestrating tissue growth are still unfolding. Here, we identify lymphatic capillaries as critical SC-niche components. In skin, lymphatics form intimate networks around hair follicle (HF) SCs. When HFs regenerate, lymphatic-SC connections become dynamic. Using a mouse model, we unravel a secretome switch in SCs that controls lymphatic behavior. Resting SCs express angiopoietin-like protein 7 *(Angptl7),* promoting lymphatic drainage. Activated SCs switch to *Angptl4,* triggering transient lymphatic dissociation and reduced drainage. When lymphatics are perturbed or the secretome switch is disrupted, HFs cycle precociously and tissue regeneration becomes asynchronous. In unearthing lymphatic capillaries as a critical SC-niche element, we have learned how SCs coordinate their activity across a tissue.

To replenish and repair the tissues in which they reside, stem cells (SCs) must not only self-renew but also generate differentiated lineages on demand (1). Their interactions with their



[*]**Corresponding author.** fuchslb@rockefeller.edu.

Author contributions:

S.G.-C. and E.F. conceptualized the study, designed the experiments, and wrote the manuscript. H.Y. helped with cloning strategies, analyzed sequencing data, and contributed to lymphatic-depletion experiments. S.C.B performed and analyzed in vitro experiments. Y.M. performed and analyzed immune profiling. J.L. performed in utero lentiviral injections. R.P.K., X.L., and B.J.M. helped with mouse models and contributed to lymphatic-related in vitro assays. J.C.-R. helped with skin sections. S.G.-C. performed all other experiments. E.F. supervised the project.

Competing interests:

B.J.M. is an inventor on patent application number 62112273, submitted by Memorial Sloan Kettering Cancer Center, that covers the treatment of lymphedema with topical formulations.

Data and materials availability:

All materials are available by material transfer agreements. Newly generated data have been deposited in NCBI's GenBank, and their accession numbers are listed in table S3.

microenvironment influence this decision (2–4). SC-niche interactions must be tightly regulated to avoid either excessive SC activity, which can cause tissue overgrowth and SC exhaustion, or in-sufficient activity, which can contribute to aging and defective tissue regeneration (5).

Despite the importance of niche constituents, SC-niche cross-talk is poorly understood. Additionally, most tissues have multiple niches, and the field still lacks an understanding of how SC niches are coordinated across a tissue. To tackle these problems, we used the murine hair coat as our paradigm because hair follicles (HFs) proceed through synchronized cycles of active growing (anagen) and resting (telogen) phases (the “hair cycle”), fueled by SCs within an anatomical niche (“bulge”) (3,6) located just below the sebaceous glands (SGs) of every HF.

Hair growth is sensitive to systemic changes (7,8), hinting that vasculature (9) may be a key hair follicle stem cell (HFSC)-niche component. Although blood vessels are niche constituents in some tissues, whether and how lymphatic vasculature affects SC function is unclear (10–16). In this study, using cell biology, three-dimensional (3D) deep imaging, and molecular genetic approaches, we identify lymphatic capillaries as an intimate feature of the HFSC niche. We show that dynamic lymphatic remodeling, driven by SCs, regulates the regenerative process and integrates SC niches across the tissue.

## Lymphatic capillaries: A newly identified SC-niche component

Assessing vascular-SC spatial relationships was made possible by a recent clearing method that renders opaque tissue transparent while preserving cellular and subcellular tissue structures (17) (fig. S1A). Whole-mount immunofluorescence and 3D image reconstruction of skin exposed an array of dermal vessels, positive for panendothelial marker CD31, just below HF SGs. During telogen, large-diameter vessels closely approached keratin 24 ($KRT24^+$) HFSCs within the lower bulge (fig. S1B and movie S1).

HFSC-associated vessels were not blood vessels ($Endomucin^+$), but rather they were positive for both surface lymphatic vessel endothelial hyaluronan receptor-1 (LYVE1) and vascular endothelial growth factor tyrosine kinase receptor-3 (VEGFR3), establishing their lymphatic endothelial identity (Fig. 1, A and B; fig. S1, C to G; and movies S2 to S5). A similar association between lymphatic capillaries and the bulge was seen in human HFs, which spend most of their time in anagen (fig. S1H). We focused on mice, whose hair growth cycles are shorter and temporally choreographed. By studying telogen (Tel), it was clear that lymphatics were tightly associated with the bulge and, to a lesser extent, with progenitors (hair germ, HG) that are primed to undergo proliferation and fate commitment at the onset of tissue regeneration [anagen I (AnaI)] (1) (Fig. 1A and fig. S1I).

Lymphatic capillaries drain into collecting vessels, which differ molecularly and anatomically, as well as in terms of permissiveness to fluid and cell entry (18). Lymphatics associated with the HFSC niche were thin-walled and blind-ended lymphatic capillaries ($VEGFR3^+LYVE1^+$), whereas collecting vessels ($VEGFR3^+LYVE1^{neg}$) resided deeper within the dermis (Fig. 1, C and D, and fig. S1J). Moreover, relative to the posterior arrector

pili muscle, capillaries were asymmetrically positioned anteriorly along each bulge (fig. S1K and movie S6), at sites where new SCs form during early anagen (3). During embryogenesis, connections between lymphatic capillaries and HFs also coincided with emergence of the quiescent bulge niche (16,19) (fig. S2 and movies S7 to S11).

## Lymphatic capillaries maintain SC quiescence

To determine whether lymphatic integrity functions in HF quiescence, we perturbed the lymphatic vascular network. Using mice expressing *CreER* knocked into the *Prox-1* locus (20) and harboring *Rosa26-fl-stop-fl-YFP,* we first activated lineage-tracing in telogen skin and confirmed by immunofluorescence and flow cytometry that *Prox1-YFP*$^{+}$ cells were exclusively lymphatics (fig. S3, A to D). We then intercrossed a Cre-recombinase-inducible diphtheria toxin (DT) receptor line *(iDTR)* (21) with *Prox1-CreER* mice and induced iDTR expression during the extended second telogen.

A single DT intradermal injection induced lymphatic cell death and disrupted the network (Fig. 2A and fig. S3, E to H). This perturbation stimulated HFs to proliferate and enter anagen, irrespective of targeting lymphatics in first or second telogen or even early anagen (Fig. 2, B and C, and fig. S4). Anagen entry did not induce *Prox1* expression in HFSCs, blood capillaries remained intact, and the skin immune cell milieu resembled normal telogen-to-anagen transition (22) (figs. S4 and S5).

To further assess whether precocious HFSC proliferation might arise directly from disrupting the lymphatic-SC niche network, we administered soluble VEGFR3 receptor intradermally during second telogen. Because VEGFR3 signaling is essential for lymphatic endothelial cell proliferation and survival, its interception causes lymphatic regression (23). Notably, precocious HF anagen entry was recapitulated with this model (Fig. 2D and fig. S6). Given that VEGFR3 (*Flt4*) was expressed by lymphatics and not HFSCs (fig. S4D), these data further underscored a role for lymphatic capillaries in HF regeneration.

## The lymphatic-SC niche is dynamic during physiological regeneration

Shortly after hair cycle onset (AnaII to AnaIII) in normal skin, LYVE1$^{+}$PROX1$^{+}$VEGFR3$^{+}$ lymphatic capillaries exhibited signs of remodeling around the SC niche (Fig. 3A and fig. S7A). Although capillaries still connected to underlying PROX1$^{+}$VEGFR3$^{+}$LYVE1$^{neg}$ collecting vessels and maintained cell numbers with little or no signs of apoptosis, they were dissociated from SC niches and dilated (Fig. 3, B to D; fig. S7, B and C; and movie S12). This dissociation was transient, and by AnaIV, lymphatics resumed their niche connection.

Given the well-established role of lymphatic vessels in controlling tissue fluid balance and macromolecule efflux (18,24), we also assessed their drainage during hair regeneration. After intradermal injections, both Evans blue dye clearance (25) and OVA-Ax488 drainage into brachial lymph nodes were significantly delayed during the narrow hair cycle window when lymphatics were dissociated (Fig. 3E). Morphologically, the dissociated capillaries displayed signs of reduced permeability (26, 27), with no major hair cycle-associated changes in blood vessel permeability (fig. S7, D and E). When fluid volume was artificially

overloaded in skin, HFSCs precociously proliferated (fig. S7F), which is consistent with a role for transient lymphatic dilation in HF regeneration.

Although we cannot exclude the possibility that mechanical forces imposed by HF regeneration might influence SC-lymphatic dynamics, HFs were still growing downward after lymphatic-SC niche connections were restored. However, this timing did coincide with the return of bulge SCs to quiescence (4). Based on these considerations, lymphatic-SC connections seemed to be affecting HFSC behavior, but by mechanisms beyond HF downgrowth. Although outside the scope of this work, possibilities include draining proliferation stimuli (growth factors, metabolites, toxins) from the SC niche or, alternatively, producing inhibitory factors that keep HFSC self-renewal in check.

## A lymphovascular switch at the onset of SC activation

When transplanted in vivo, cultured HFSCs can establish cycling HFs (1), suggesting that SCs participate in organizing their niche. This led us to speculate that HFSCs might be orchestrating lymphatic capillary connections. To address this possibility, we began by purifying and transcriptome-profiling HFSCs during (i) telogen, when SCs are quiescent and lymphatics are associated; and (ii) AnaII-III, when SCs are proliferative and lymphatics are dissociated (fig. S8A).

Established proangiogenic and lymphangiogenic factors, such as *Vegfa, Vegfb,* and *Vegfc,* showed little or no expression in either quiescent or proliferative bulge SCs and hence were unlikely to control bulge-lymphatic dynamics (Fig. 4A). Changes in stromal VEGFC expression and/or processing were also not detected during this time (fig. S8, B and C). Moreover, although a VEGFC gradient is known to elicit robust lymphatic VEGFR3-mediated sprouting, overt signs of enhanced sprouting were absent (fig. S7). Thus, SC-lymphatic dynamics appeared to be controlled by other factors.

A number of putative vascular regulators displayed expression patterns paralleling these dynamics. Most notably, *Angptl7* was expressed in telogen bulge SCs, whereas *Angptl4* and netrin-4 *(Ntn4)* were induced in AnaII-III bulge SCs concomitant with *Angptl7* down-regulation (Fig. 4A). These factors appeared to be bulge-specific (Fig. 4B).

Focusing first on *Angptl7,* we find that prior RNA sequencing (RNA-seq) data (28) showed that *Angptl7* was not even expressed in the primed HG cells of telogen or early anagen HFs (Fig. 4C and fig. S8D). To delineate the detailed temporal changes of *Angptl7* within bulge SCs, we performed stage-specific single-cell RNA-seq. Three distinct temporal patterns emerged from t-distributed stochastic neighbor embedding (t-SNE) and unsupervised hierarchical clustering (Fig. 4D and fig. S8E). Using machine learning-based cell-cycle allocation analysis (29), it was concluded that proliferative cells resided in AnaII SCs, in agreement with our 5-ethynyl-2'-deoxyuridine (EdU) labeling studies. Additionally, in contrast to SC marker *Sox9,* which was maintained in bulge SCs at all stages, *Angptl7* transcription in bulge SCs diminished shortly after anagen onset, even sooner than that of established quiescence regulator *Nfatc1* (28). Moreover, the *Angptl7* expression dip was transient, occurring only between AnaII and AnaIII (Fig. 4E).

*Angptl7* dynamics were recapitulated at the chromatin level. As judged by chromatin immunoprecipitation sequencing (ChIP-seq) analyses of fluorescence-activated cell sorting (FACS)-purified HF cells (30), the *Angptl7* chromatin state was active in telogen (H3K27ac$^{+}$), poised in AnaIII (H3K27ac$^{neg}$H3K4me1$^{+}$), and silent in AnaVI differentiated cells (H3K27ac$^{neg}$H3K4me1$^{neg}$) (fig. S9A). Moreover, when either of the two *Angptl7* locus-accessible chromatin elements (30) were used as enhancers to drive enhanced green fluorescent protein *(eGFP)* expression in vivo, reporters faithfully recapitulated *Angptl7*'s temporal dynamics in bulge expression during the hair cycle (Fig. 4F and fig. S9B). These results intimated that changes in SC-derived *Angptl7* transcription are involved in reshaping the regenerative microenvironment of the niche.

## A SC-driven secretome switch is required for lymphatic remodeling

Angiopoietin-like (ANGPTL) proteins do not bind to classical angiopoietin receptors, and knowledge of these orphan ligands is still scant (31, 32). To address whether *Angptl7* down-regulation functions in HFSC activation, we engineered mice to harbor an *Angptl7* transgene that is selectively doxycycline-inducible in skin progenitors (33). We then induced at telogen and examined the consequences of maintaining ANGPTL7 through early stages of the newly entered hair cycle (fig. S10, A to E).

In contrast to the lymphatic-SC niche remodeling of normal HFs, lymphatic capillaries remained tightly associated and the bulge remained quiescent when *Angptl7* was sustained (Fig. 5A). Consistent with a nonautonomous role for ANGPTL7 in controlling stemness activity, recombinant ANGPTL7 did not appreciably alter colony formation of HFSCs in vitro. Rather, concomitant with sustained lymphatic efflux and drainage capacity, entry into the hair cycle was markedly delayed (Fig. 5B and fig. S10, C to E). Because a role for ANGPTL7 in angiogenesis had been suggested, we looked for, but did not find, perturbations in blood vessel density and coverage in our *Angptl7*-induced skin (fig. S10E). ANGPTL7 overexpression also did not affect levels of CCBE1, a protein required for VEGFC-mediated lymphangiogenesis (fig. S10F).

Because the hair cycle was delayed upon sustaining *Angptl7,* we wondered whether ANGPTL7 dynamics might be important for other regenerative responses. We focused on hair plucking (waxing), as it mechanically perturbs the SC niche, generating a wound-like response (3,34). Plucking not only activated hair regeneration, as expected, it also restricted lymphatic drainage and disrupted lymphatic-SC associations (fig. S11, A and B). Moreover, when *Angptl7* was sustained, wound-induced hair regeneration was abrogated; conversely, after skin injury in a normal setting, *Angptl7* gene expression plummeted (fig. S11, C and D).

Turning to the flip side of the secretome switch, we engineered doxycycline-inducible versions of *Angptl4.* When induced in telogen, ANGPTL4 precociously disrupted lymphatic capillaries surrounding the bulge, reducing lymphatic drainage and activating HFSCs (Fig. 5, C and D, and fig. S12). Despite a purported role for ANGPTL4 in blood vasculature (35), endothelial vessel density was largely unchanged, both in AnaII-III of the normal hair cycle

and in telogen of the *Angptl4-induced* hair cycle. Similar results were obtained with NTN4, previously implicated in endothelial cell biology (36–38) (fig. S12).

Our data suggested that the HFSC-derived secretome can influence lymphatic dynamics directly, which we tested by evaluating lymphatic tube formation in a 3D-Matrigel system. Formation of tubelike structures was enhanced with ANGPTL7 and impaired with ANGPTL4, supporting this hypothesis. Consistent with a nonautonomous role, SC-driven factors in vitro neither affected HFSC growth nor stimulated immune cell migration (fig. S13).

Although ANGPTL and NTN receptors are poorly studied, transcriptional landscaping of freshly isolated endothelial cells from skin revealed preferential expression of their putative receptors by the lymphatic vessels (fig. S14A). Telogen-associated lymphatic capillaries also preferentially expressed WNT inhibitors. As WNT signaling is critical for HFSC activation and hair cycling (30, 39), these correlations are suggestive of an additional layer of regulation by which lymphatic capillaries might coordinate SC regeneration.

Single-cell analyses of lymphatic capillary cells isolated and characterized from telogen and from anagen skins revealed similar transcriptomic patterns, with only 4 to 5% of mRNAs changed temporally by >2× (fig. S14B). Of these genes, the most notable changes appeared to be in lymphatic tube formation and fluid dynamics. Thus, if capillary growth factors participate in maintaining HFSC quiescence, their significance likely resides in the dynamic regulation of lymphatic-SC connections rather than their differential transcription during the hair cycle.

## A role for the lymphatic network in integrating SC-niche behavior across a tissue

Turning to the physiological relevance of the SC-lymphatic connection, we used our powerful in utero lentiviral delivery method to selectively and efficiently knock down *Angptl7* in skin progenitors with one of two different short hairpin RNAs (shRNAs). When *Scramble* controls were in telogen, *shAngptl7* HFs had already entered anagen. Full anagen follicles were interspersed with telogen ones, indicating hair cycle asynchrony (Fig. 6A and fig. S15A).

The failure of HFSCs to generate ANGPTL7 profoundly affected lymphatic biology. Lymphatics were discontinuous and abnormally dilated, and they displayed impaired drainage, as judged both functionally and morphologically (Fig. 6B and fig. S15B). This chronic lymphatic dysfunction was associated with HF hyperplasia and reduced bone morphogenetic protein (BMP)/pSMAD1/5/9 signaling, which are essential for maintaining SC quiescence (3) (Fig. 6, B and C; fig. S15C; and movie S13). Hyperplastic HFs were associated with the most highly dilated lymphatic capillaries, which maintained their identity but displayed reduced drainage (Fig. 6, B and D; fig. S15D; and movie S14). Blood vessel density was also increased at hyperplastic HFs (fig. S15E and movie S15), although this was unlikely to have driven lymphatic remodeling, given that SCs associated primarily with lymphatic capillaries in normal homeostasis.

The asynchrony across the hair coat did not appear to stem from variations in transgene integration, as this would have generated clonal patches of HFs at specific cycle stages, which we did not see. However, to unequivocally demonstrate that HF asynchrony arose from perturbations in the SC-lymphatic crosstalk, and not our lentiviral delivery method, we used *Flt4*$^{Chy}$ mice, which harbor a mutant *Vegfr3* allele, creating VEGFR3 dimers with dysfunctional tyrosine kinase activity and dysfunctional lymphatics (40). *Flt4*$^{Chy}$ mice recapitulated the asynchrony of bulge-SC niches, accompanied with dysfunctional lymphatic vessels (Fig. 6E and fig. S15, F and G). Taken together, these data underscore the importance of lymphatic capillary dynamics, driven by SCs, in integrating SC-niche behavior across a tissue.

## Lymphatic capillaries as a dynamic SC-niche newcomer that coordinates SC behavior

The niche microenvironments of quiescent SCs, such as those of bone marrow, muscle, and HFs, provide the input signals that keep these SCs in an undifferentiated, inactive state (41). Niche-SC interactions must be dynamic in order to mobilize SCs to regenerate tissues. Additionally, SCs have an intrinsic ability to communicate with their neighbors and reshape their niche (34).

Our study identifies lymphatic capillaries as dynamic SC-niche elements that integrate SC niches and synchronize SC behavior across the hair coat. We have learned that, to mobilize HFSCs for either normal regenerative demands or those induced by injury, these SCs undergo a secretome switch that triggers transient dissociation of lymphatics from the niche (Fig. 6F).

Although the possible ways by which lymphatics control HFSCs are numerous, and the communication circuits are likely complex, our genetic manipulations of the lymphatic-SC niche connection underscore its functional importance in balancing SC self-renewal and quiescence. Indeed, as soon as bulge SCs launch production of their committed proliferative progeny and self-renew, the lymphatic capillaries resume connections with their SC neighbors, and niche quiescence is restored. The process is a two-way street, because the dynamic remodeling of lymphatic capillaries is orchestrated by bulge SCs, whereas the lymphatics govern SC behavior.

Drainage of tissue interstitial fluids and macromolecules has been a subject of interest for decades. We have unearthed a need to balance cutaneous influx of fluids and macromolecules in controlling SC behavior. Future studies will be needed to dissect the impact of interstitial fluid composition, extracellular macromolecule dynamics, and immune cell efflux on stem cell biology. Additionally, short remodeling duration suggests that lymphatic dissociation from the SC niche may be deleterious, perhaps rendering SCs transiently vulnerable to toxins or increased fluid pressure.

Our discovery that lymphatics localize to both mouse and human HFSC niches suggests that the need to establish such connections is not only physiologically important but also evolutionarily conserved, raising the possibility that lymphatic capillaries may participate in

other SC niches to meet their specialized regenerative demands. With our newfound understanding of skin SC-lymphatic interactions, it now merits addressing whether the stem cell exhaustion that accompanies wound-healing defects and hair loss in aging and in patients with lymphedema (24,42) might be rooted in decline of lymphatics and interstitial fluid draining. If such links exist, targeting lymphatic function could prove to be a promising preventative therapeutic target for hair loss and wound repair.

## Supplementary Material

Refer to Web version on PubMed Central for supplementary material.

## ACKNOWLEDGMENTS

We thank The Rockefeller University's FACS facility (S. Mazel); Rockefeller's and Weill Cornell's high-throughput sequencing facilities; K. Minkis (Weill Cornell) for human biopsies; and G. Oliver (Northwestern), M. Gunzer (Univ. of Duisburg-Essen), G. Zarkada (Yale), and P. Rajasethupathy, P. Cohen, S. Shaham, and G. D. Victora (Rockefeller) for discussions. We thank the Fuchs laboratory for technical assistance (N. Gomez, I. Matos, K. Lay, B. Hurwitz, M. ElJaby, E. Wong, and M. Nikolova); mouse handling and experiments (M. Sribour, L. Hidalgo, and L. Polak); anti-KRT24 antibody (E. Wong); and discussions (S. Liu, F. Garcia Quiroz, S. Naik, Y. Ge, M. Laurin, S. Ellis, V. Fiore, K. Gonzales, R. C. Adam, and R. E. Niec).

Funding:

S.G.-C. received postdoctoral support from the Human Frontier Science Program (LT001519/2017), EMBO (ALTF 1239–2016), and the Revson Foundation. E.F. is an HHMI investigator. S.C.B. received predoctoral support from the National Cancer Institute (F31CA236465) and the Tri-Institutional Medical Scientist Training Program (T32GM007739). This work was supported by NIH grants R01-AR050452 and R01-AR31737 to E.F.

## REFERENCES AND NOTES

1. Gonzales KAU, Fuchs E, Dev. Cell 43, 387–401 (2017). [PubMed: 29161590]
2. Li L, Clevers H, Science 327, 542–545 (2010). [PubMed: 20110496]
3. Hsu YC, Li L, Fuchs E, Nat. Med 20, 847–856 (2014). [PubMed: 25100530]
4. Morrison SJ, Spradling AC, Cell 132, 598–611 (2008). [PubMed: 18295578]
5. Ge Y, Fuchs E, Nat. Rev. Genet 19, 311–325 (2018). [PubMed: 29479084]
6. Plikus MV et al., Nature 451, 340–344 (2008). [PubMed: 18202659]
7. Festa E. et al., Cell 146, 761–771 (2011). [PubMed: 21884937]
8. Goldstein J. et al., Genes Dev. 28, 983–994 (2014). [PubMed: 24732379]
9. Durward A, Rudall KM, in The Biology of Human Hair Growth (Academic Press, 1958), pp. 189–218.
10. Tamplin OJ et al., Cell 160, 241–252 (2015). [PubMed: 25594182]
11. Kiel MJ et al., Cell 121, 1109–1121 (2005). [PubMed: 15989959]
12. Kunisaki Y. et al., Nature 502, 637–643 (2013). [PubMed: 24107994]
13. Tavazoie M. et al., Cell Stem Cell 3, 279–288 (2008). [PubMed: 18786415]
14. Tang W. et al., Science 322, 583–586 (2008). [PubMed: 18801968]
15. Yoshida S, Sukeno M, Nabeshima Y, Science 317, 1722–1726 (2007). [PubMed: 17823316]
16. Pena-Jimenez D. et al., EMBO J. 38, e101688 (2019).
17. Richardson DSS, Lichtman JWW, Cell 162, 246–257 (2015). [PubMed: 26186186]
18. Alitalo K, Tammela T, Petrova TV, Nature 438, 946–953 (2005). [PubMed: 16355212]
19. Nowak JA, Polak L, Pasolli HA, Fuchs E, Cell Stem Cell 3, 33–43 (2008). [PubMed: 18593557]
20. Srinivasan RS et al., Genes Dev. 21, 2422–2432 (2007). [PubMed: 17908929]
21. Buch T. et al., Nat. Methods 2, 419–426 (2005). [PubMed: 15908920]

22. Ali N. et al., Cell 169, 1119–1129.e11 (2017).
23. Mäkinen T. et al., Nat. Med 7, 199–05 (2001). [PubMed: 11175851]
24. Da Mesquita S. et al., Nature 560, 185–191 (2018). [PubMed: 30046111]
25. Huggenberger R. et al., Blood 117, 4667–4678 (2011). [PubMed: 21364190]
26. Baluk P. et al., J. Exp. Med 204, 2349–2362 (2007). [PubMed: 17846148]
27. Zhang F. et al., Science 361, 599–603 (2018). [PubMed: 30093598]
28. Yang H, Adam RC, Ge Y, Hua ZL, Fuchs E, Cell 169, 483–496.e13 (2017).
29. Scialdone A. et al., Methods 85, 54–61 (2015). [PubMed: 26142758]
30. Adam RC et al., Cell Stem Cell 22, 398–413.e7 (2018).
31. Zhang CC et al., Nat Med. 12, 240–245 (2006). [PubMed: 16429146]
32. Zheng J. et al., Nature 485, 656–660 (2012). [PubMed: 22660330]
33. Beronja S, Livshits G, Williams S, Fuchs E, Nat. Med 16, 821–827 (2010). [PubMed: 20526348]
34. Blanpain C, Lowry WE, Geoghegan A, Polak L, Fuchs E, Cell 118, 635–648 (2004). [PubMed: 15339667]
35. Backhed F, Crawford PA, O'Donnell D, Gordon JI, Proc. Natl. Acad. Sci. U.S.A 104, 606–611 (2007). [PubMed: 17202268]
36. Lu X. et al., Nature 432, 179–186 (2004). [PubMed: 15510105]
37. Wilson BD et al., Science 313, 640–644 (2006). [PubMed: 16809490]
38. Cirulli V, Yebra M, Nat. Rev. Mol. Cell Biol 8, 296–306 (2007). [PubMed: 17356579]
39. Lien WH et al., Nat. Cell Biol 16, 179–190 (2014). [PubMed: 24463605]
40. Karkkainen MJ et al., Proc. Natl. Acad. Sci. U.S.A 98, 12677–2682 (2001).
41. Morrison SJ, Scadden DT, Nature 505, 327–334 (2014). [PubMed: 24429631]
42. Karaman S. et al., Angiogenesis 18, 489–498 (2015). [PubMed: 26260189]

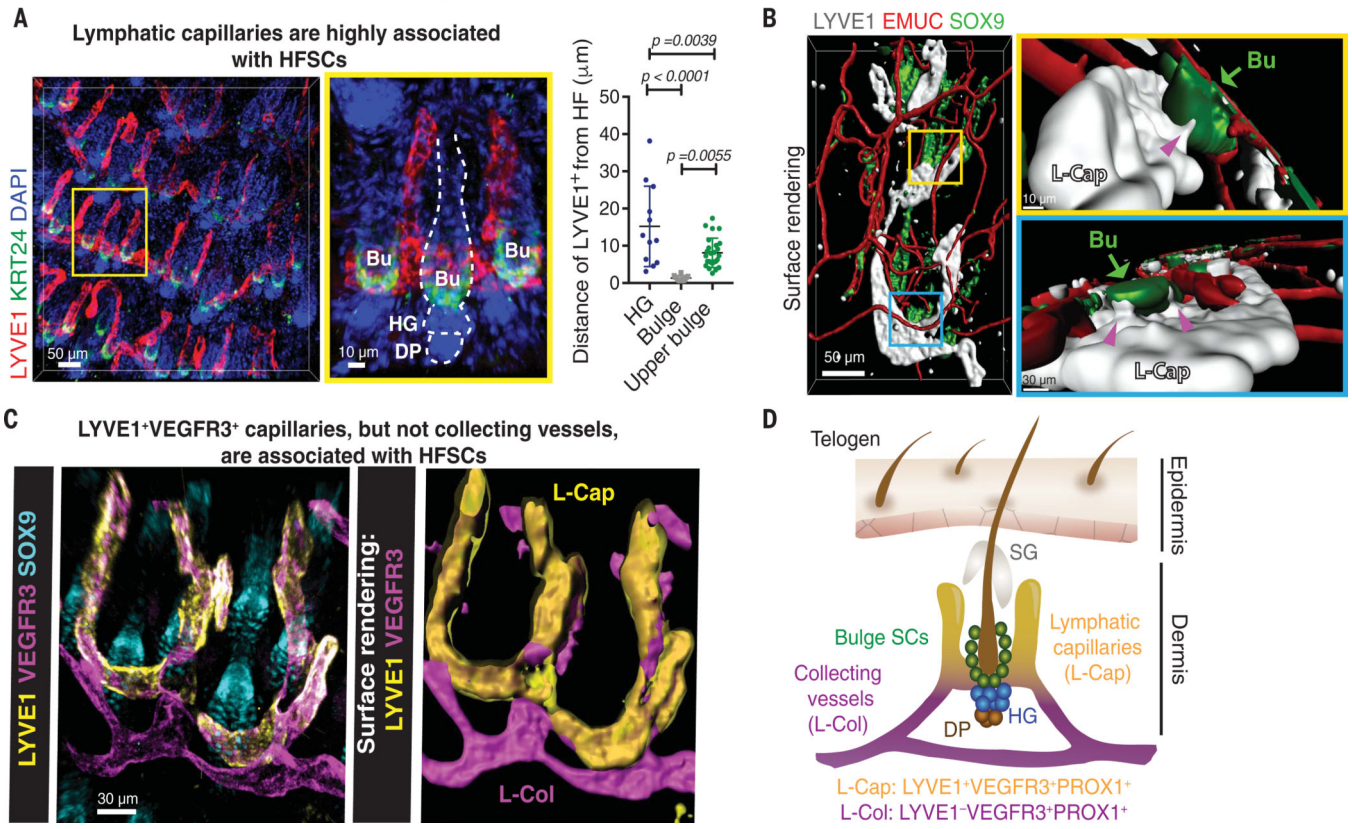


**Fig. 1. Lymphatic capillaries tightly associate with HFSCs.**

(**A**) 3D image and quantifications demonstrating LYVE1$^{+}$ lymphatic capillaries around telogen HF bulges (KRT24$^{+}$; boxed image enlarged at right) [$n$ = 4 mice; multiple measurements per mouse; one-way analysis of variance (ANOVA); Tukey's multiple comparisons test]. DAPI, 4',6-diamidino-2-phenylindole. (**B**) Surface renderings of SOX9$^{+}$ bulges, LYVE$^{+}$ lymphatic capillaries, and Endomucin$^{+}$ (EMUC) blood capillaries (90°-angle views of boxed images are enlarged at right). (**C**) Lymphatic capillaries (L-Cap; LYVE1$^{+}$VEGFR3$^{+}$) but not collecting vessels (L-Col; LYVE1$^{neg}$VEGFR3$^{+}$) associate with telogen SOX9$^{+}$ bulge SCs. (**D**) Schematic of SC-lymphatic association at telogen. Bu, bulge; HG, hair germ; DP, dermal papilla; SG, sebaceous gland.

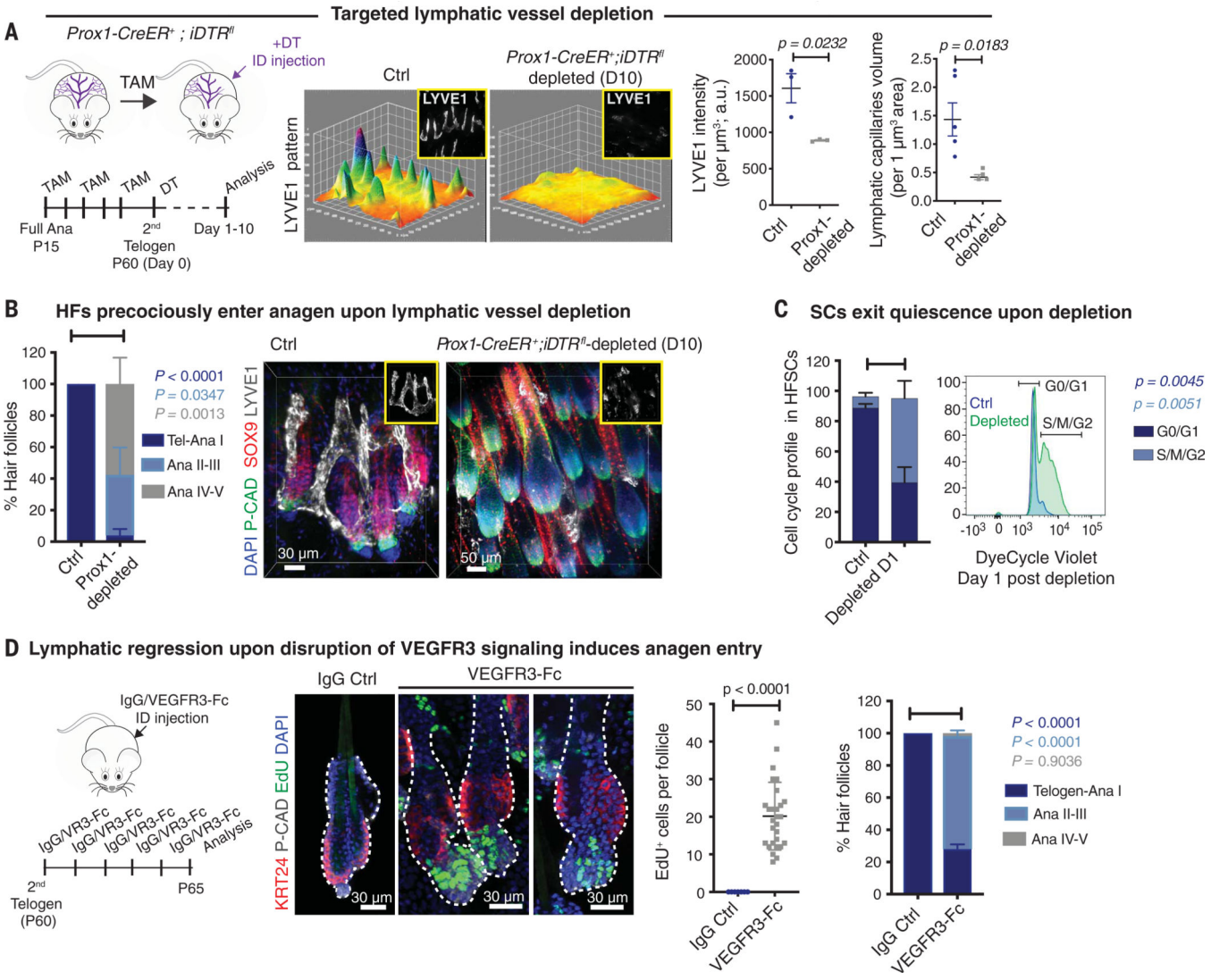


**Fig. 2. Disrupting lymphatic capillaries triggers hair regeneration.**

(**A**) Timeline of experimental model and diphtheria toxin (DT)-induced depletion of lymphatic vessels during the long quiescence of second telogen. Quantifications: lymphatic intensity ($n = 3$); volume ($n = 5$ and 4 for Ctrl and *Proxl*-depleted, respectively; two-tailed unpaired *t* test). ID, intradermal; TAM, tamoxifen; P, postnatal day; Ctrl, control; D, day; a.u., arbitrary units. (**B**) Precocious anagen induction after lymphatic depletion, as demonstrated by HF growth and association with LYVE1$^+$ capillaries ($n = 5$, two-way ANOVA with Sidak's multiple comparisons test). P-CAD, P-cadherin. (**C**) Flow cytometry of HFSC cell cycle after lymphatic depletion ($n = 3$, two-way ANOVA with Sidak's multiple comparisons test). (**D**) Experimental strategy using decoy VEGF3-Fc to interrupt VEGFR3 signaling in dermal lymphatic vessels. EdU incorporation reveals anagen entry after treatment ($n = 4$, multiple EdU measurements, two-tailed unpaired *t* test). IgG, immunoglobulin G.

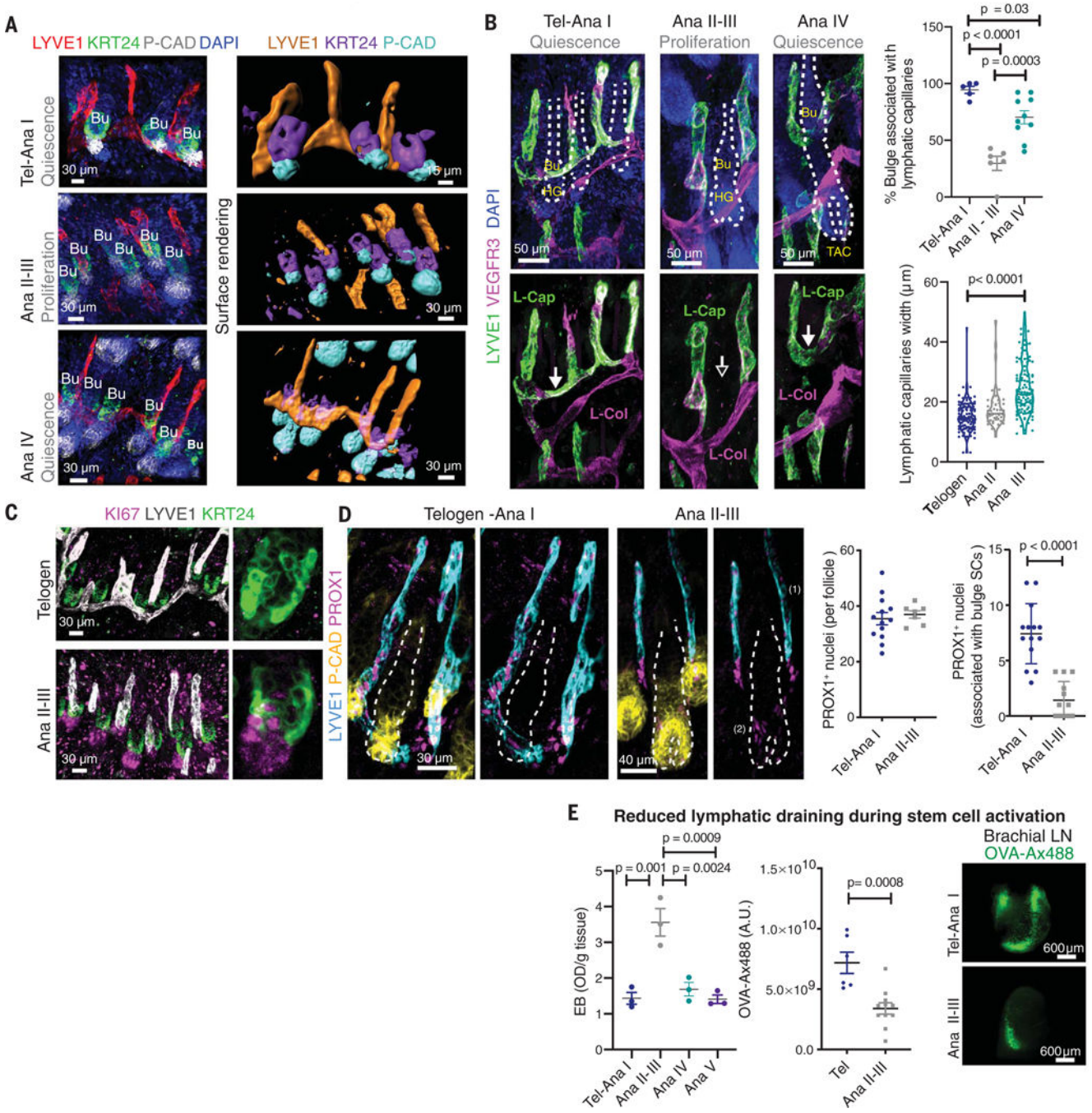


**Fig. 3. HFSC-lymphatic associations are dynamic.**

(**A**) 3D imaging and surface rendering of cleared skin tissue, demonstrating LYVE1$^{+}$ lymphatic capillary dissociation from KRT24$^{+}$ bulge SCs during AnaII—III of the hair cycle. P-CAD$^{high}$ cells are HFSC progeny. (**B**) Despite dissociating (empty arrow for dissociation versus white arrow for association) from the SC niche, lymphatic capillaries remain connected to their underlying collecting vessels (LYVE1$^{neg}$VEGFR3$^{+}$) during AnaII—III. Quantifications of temporal changes in SC-capillary associations and lymphatic width ($n$ = 5, 6 and $n$ = 5, one-way ANOVA; Tukey's multiple comparisons test). TAC, transient

amplifying cells. (**C**) Capillary dissociation correlates with bulge SC self-renewal ($Ki67^+$). (**D**) $PROX1^+$ lymphatics dissociate from the bulge during AnaII-III but do not disappear (1 indicates $Prox1^+$capillaries, 2 indicates $Prox1^+$collecting; $n = 3$; two-tailed unpaired *t* test). (**E**) Reduced lymphatic drainage capacity in AnaII—III, as measured by intradermal injections of Evans Blue (EB; $n = 3$, one-way ANOVA; Tukey's multiple comparisons test) and OVA-Ax488 efflux to brachial lymph nodes (LN; $n = 3$ and 6 for Tel-AnaI and AnaII—III, respectively; two-tailed unpaired *t* test). OD, optical density.

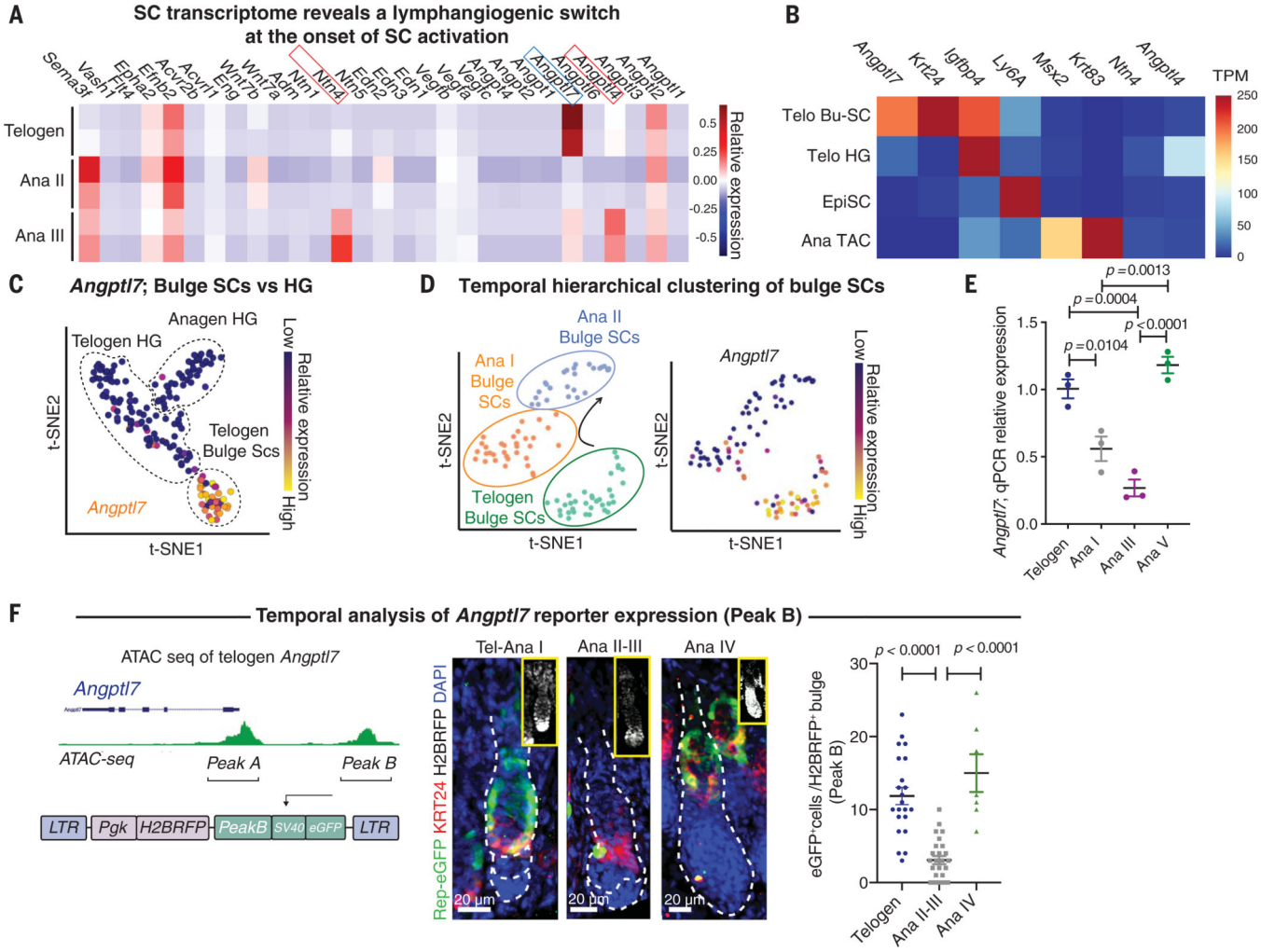


**Fig. 4. HFSCs promote a lymphovascular switch at hair regeneration onset.**

(**A**) Heatmaps of FACS-purified bulge SCs from telogen, Anall, and Analll HFs. Boxed transcripts are markedly down (blue) or up (red) upon HFSC activation. (**B**) Transcripts per million (TPM) heatmap showing paucity of *Angptl7, Angptl4,* and *Ntn4* in SCAl$^{+}$epidermal SCs (EpiSCs) or HFSC progeny (MSK2$^{+}$Krt83$^{+}$ TACs; lGBP4$^{+}$ KRT$^{neg}$ HGs). (**C** and **D**) Single-cell transcriptome clustering of (C) telogen bulge SCs, telogen HG cells, and Anal HG cells (28); and (D) telogen, Anal, and Anall bulge SCs. Each cell is represented as a dot. (**E**) Quantitative polymerase chain reaction (qPCR) validation of temporal *Angptl7* expression in bulge SCs ($n$ = 3, one-way ANOVA; Tukey's multiple comparisons test). (**F**) Accessible *Angptl7* locus telogen bulge SC chromatin peaks (left) were used to drive *eGFP* in mice. Peak B *eGFP* dynamics (right) mirror temporal *Angptl7* transcriptome changes ($n$ = 5, 5, and 3 mice analyzed for Telogen, AnaII—III, and AnaIV, respectively; one-way ANOVA; Tukey's multiple comparisons test). ATAC seq, assay for transposase-accessible chromatin using sequencing; LTR, long terminal repeats; Pgk, phosphoglycerate kinase promoter; H2BRFP, histone H2B red fluorescent protein; SV40, minimal simian virus 40 promoter; Rep-eGFP, reporter-enhanced green fluorescent protein.

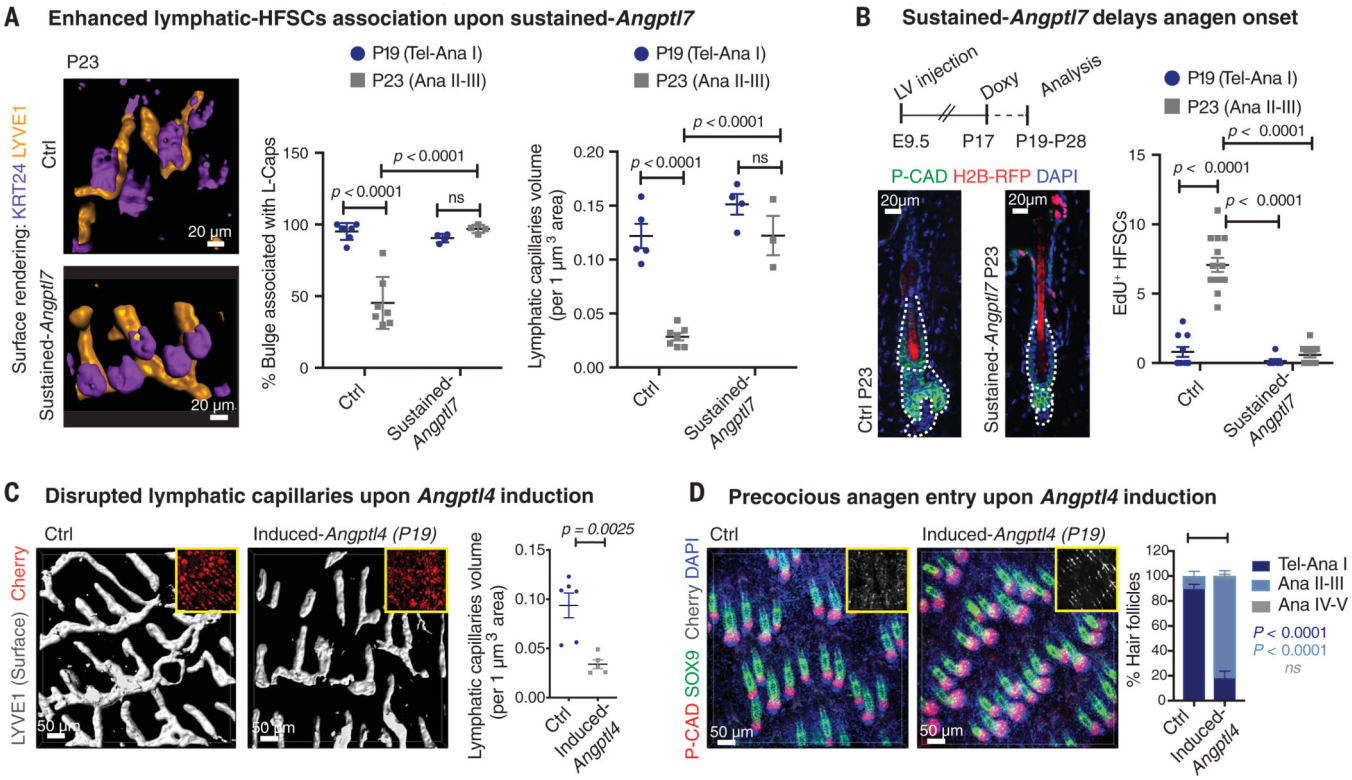


**Fig. 5. SC secretome switch promotes lymphatic remodeling.**

(**A**) (Left) Lymphatic-bulge SC connections and quantifications ($n = 7$ $rtTA^{neg}$ control; $n = 4$ $rtTA^{+}$ sustained-*Angptl7*). (Right) Capillary volumes ($n \geq 4$ per condition per genotype; two-way ANOVA; Tukey's multiple comparisons test). ns, not significant. (**B**) Doxycycline-induced *Angptl7* delays anagen onset and bulge-SC proliferation ($n = 4$ per condition per genotype; two-way ANOVA; Tukey's multiple comparisons test). E, embryonic day. (**C** and **D**) Induced *Angptl4* in telogen causes reduced lymphatic capillary density ($n \geq 5$ per condition per genotype, two-tailed unpaired *t* test) and precocious anagen entry ($n \geq 3$ per condition per genotype, two-way ANOVA with Sidak's multiple comparisons test).

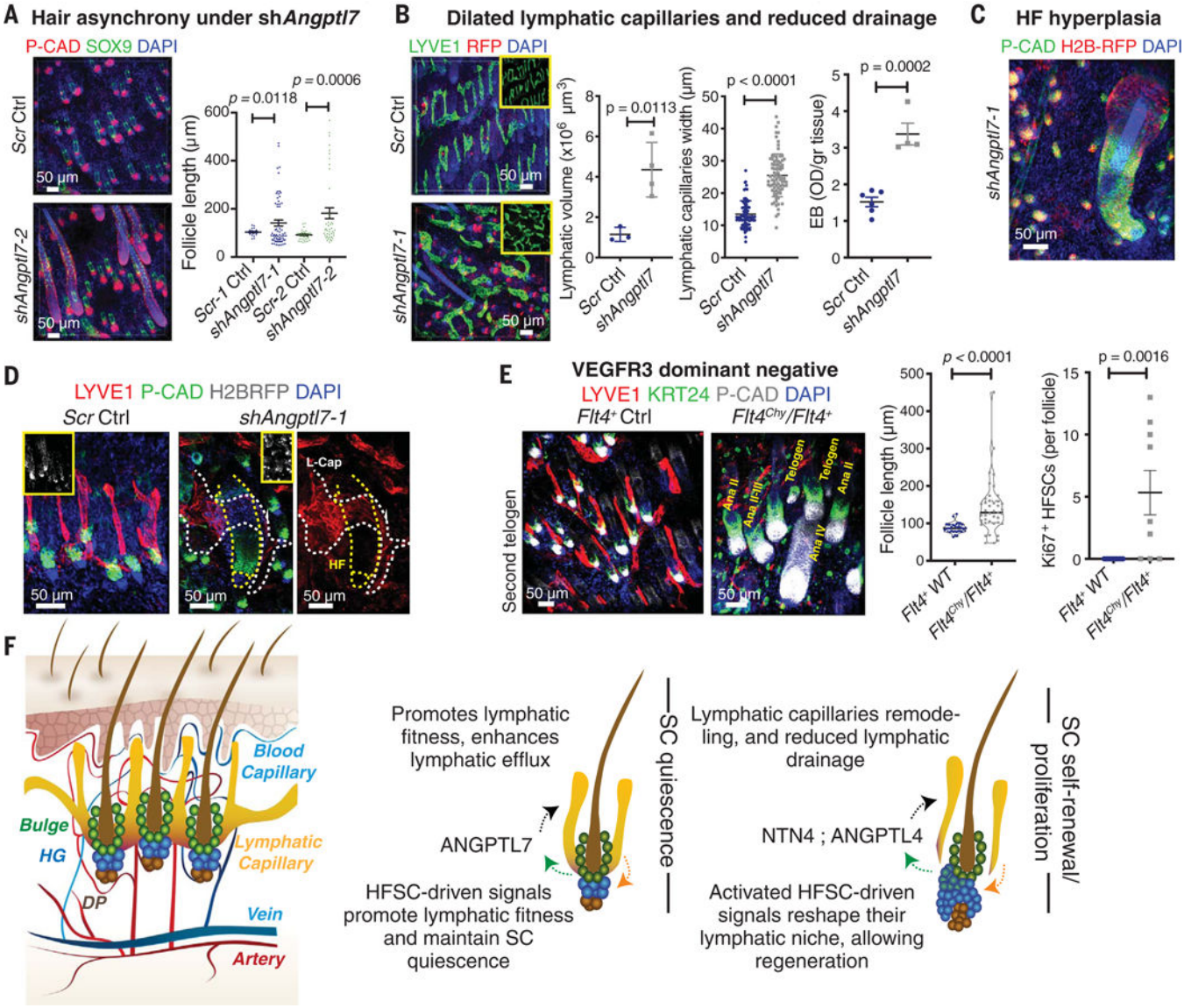


**Fig. 6. Secretome switch integrates lymphatic-SC niches across the tissue.**

(**A**) *shAngptl7* knockdown results in HF asynchrony by P19 ($n = 4$ per condition per shRNA, one-way ANOVA with Dunnett's multiple comparisons test). (**B**) *shAngptl7* in HFSCs causes lymphatic capillary dilation ($n \geq 3$ per shRNA, two-tailed unpaired $t$ test). Quantifications of lymphatic drainage capacity are shown at right, as measured by Evans blue efflux ($n \geq 4$ per shRNA per measurement, two-tailed unpaired $t$ test). (**C**) HF hyperplasia after *Angptl7* knockdown and (**D**) hyperplastic HF association with the most highly dilated lymphatic capillaries. (**E**) Expressing a dominant-negative VEGFR3, *Flt4*$^{Chy}$/*Flt4*$^{+}$ mice exhibit hair-cycling asynchrony and increased proliferation at P65, when control HFs are in second telogen ($n = 3$, two-tailed unpaired $t$ test). (**F**) Model of the HFSC secretome switch.